A Multinuclear Solid-State NMR Study of Phospholipid−Cholesterol Interactions. Dipalmitoylphosphatidylcholine−Cholesterol Binary System†

Wen Guo and James A. Hamilton*

Department of Biophysics, Boston University School of Medicine, 80 East Concord Street, Boston, Massachusetts 02118

Received July 12, 1995; Revised Manuscript Received August 29, 1995®

ABSTRACT: Multinuclear (^{1}H, ^{13}C, ^{31}P) MASNMR and static solid-state ^{31}P NMR were used to study the molecular interactions between dipalmitoylphosphatidylcholine (DPPC) and free cholesterol (CHOL) in multilayers of DPPC containing 0−65 mol % CHOL with respect to total lipid at temperatures between 25 and 55 °C. ^{13}C chemical shifts and line shapes for DPPC and CHOL resonances were measured in ^{13}C MASNMR spectra. The apparent chemical shift anisotropy (CSA) of the DPPC acyl methylene resonances [$(CH_2)_n$] was calculated from the ^{1}H MASNMR spectra. CSA and line shape changes were recorded as a function of CHOL content by ^{31}P static solids and MASNMR. The presence of CHOL significantly changed the ^{13}C chemical shifts and line shapes of DPPC carbonyl carbons below or above the main transition temperature of pure DPPC. Chemical shift changes were also observed for CHOL carbons as a function of the mixing ratio, signifying a changing local environment of CHOL. For mixtures with CHOL >50 mol %, ^{13}C MASNMR detected crystalline CHOL in the monohydrate form. When the excess CHOL was in a submicroscopic crystalline form that was not readily detected by differential scanning calorimetry, or optical microscopy (but readily observed by ^{13}C MASNMR), the ^{31}P powder pattern was affected, suggesting interaction of the excess CHOL with the aqueous interface of the bilayer. These results suggest the potential of ^{13}C MASNMR for detection of crystalline CHOL in biological samples.

As a major constituent of mammalian cell membranes, free cholesterol (CHOL)[1] has been the focus of many physical studies, especially in mixtures with phospholipids, typically phosphatidylcholine. The presence of CHOL in biological membranes modulates a number of structural and functional properties of the membrane (Yeagle, 1988). The properties of CHOL in phospholipid bilayers have been extensively used in liposome industry to improve liposome−drug encapsulation capacity (Hammond et al., 1994).

CHOL is known to broaden and eventually eliminate the gel−liquid-crystalline phase transition of model saturated phospholipid bilayers, to increase (decrease) the orientational order of the liquid-crystalline (gel) phase, and to decrease (increase) the passive permeability of phospholipid bilayers in the liquid-crystalline (gel) phase (McMullen et al., 1993). Solution ^{13}C NMR studies can be used to probe phospholipid−cholesterol interactions in small unilamellar vesicles (Yeagle et al., 1975, 1977; Brainard & Cordes, 1981), but much of the potentially relevant information for membrane structure is lost because of the fast tumbling of the vesicles and the stress caused by the high curvature. Although phospholipid multilayer dispersions are not suitable for study by solution ^{13}C NMR, they are amenable to ^{2}H NMR spectroscopy (Bonmatin et al., 1990). Specific ^{2}H labeling of CHOL or phospholipids has been especially useful in the study of molecular motions and conformations of both CHOL and phospholipids (Taylor et al., 1981; Hamilton et al., 1993; Murari et al., 1986).

More recently, a detailed study of phospholipid−cholesterol multilayers over a large temperature range (0−60 °C) combining solid-state ^{13}C and ^{2}H NMR spectroscopy was reported (Huang et al., 1993). The phase diagram derived from these NMR data had substantial differences from some previously reported phase diagrams. However, the ^{13}C NMR observations were limited to the static powder pattern of the *sn*-2 carbonyl with ^{13}C=O enrichment. Information on other molecular segments was undiscovered by such isotope enrichment.

In spite of the vast number of biophysical studies of the interactions of CHOL with phospholipids, there is still controversy about many essential features of these interactions, such as precisely where CHOL is located in the phospholipid matrix and whether there are specific H-bonding interactions between CHOL and phospholipid polar groups. MASNMR appears to be a promising newer NMR approach, as it can provide very high-resolution spectra of multilamellar phospholipid/CHOL dispersions (Forbes, 1988a,b). ^{13}C MASNMR has been used to measure the chemical shift of the ^{13}C-enriched *sn*-2 carbonyl of DPPC in the presence and absence of CHOL to assess the possibility of H-bonding of this group with CHOL (Sankaram & Thompson, 1991). However, in all these prior studies, only one mixing ratio (50 mol % CHOL) was reported.

There are still few studies of high levels of CHOL in phospholipid bilayers. Crystallization of CHOL from membranes may be an important step in several pathologies involving CHOL, such as atherosclerosis (Tangirala et al., 1994; Thomson et al., 1993; Levecq et al., 1992), gallstone

† This work was supported by NIH Grant RO1 HL41904 to J.A.H. and T32 HL07224 to W.G.

* To whom correspondence should be addressed.

® Abstract published in *Advance ACS Abstracts,* October 1, 1995.

[1] Abbreviations: NMR, nuclear magnetic resonance; MAS, magic angle spinning; MASNMR, NMR with magic angle spinning; CPMAS, MASNMR with cross-polarization transfer; CHOL, free cholesterol; DMPC, 1,2-*sn*-dimyristoylphosphatidylcholine; DPPC, 1,2-*sn*-dipalmitoylphosphatidylcholine; CSA, chemical shift anisotropy; S_o, disordered gel phase; L_o, ordered liquid-crystalline phase; $L_{\beta'}$, gel phase; $P_{\beta'}$, ripple phase; L_α, liquid-crystalline phase; L_d, disordered liquid-crystalline phase; T_m, main transition temperature of DPPC.

0006-2960/95/0434-14174$09.00/0

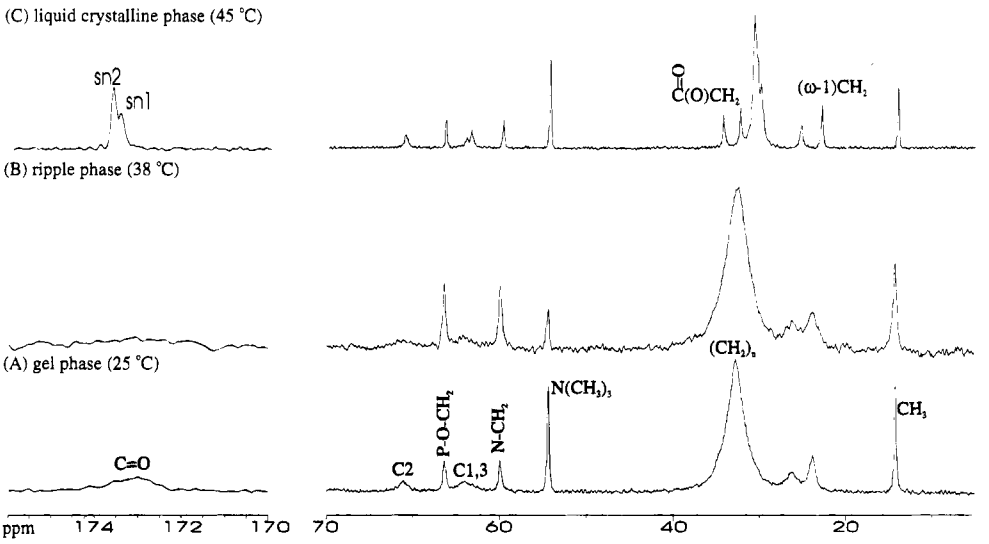

FIGURE 1: Proton-decoupled ^{13}C MASNMR spectra of fully hydrated DPPC multilayers: (A) gel phase (L_β) at 25 °C; (B) ripple phase (P_β) at 38 °C; (C) liquid-crystalline phase (L_α) at 45 °C. Spectra A and B were obtained with CPMAS, and spectrum C with MAS but without cross-polarization transfer. All spectra were obtained with a 4 kHz MAS spinning rate; 2K data points were zero-filled to 8K, and spectra were processed with 3 Hz line broadening. Selected resonances are labeled: *sn*-1 and *sn*-2 carbonyls (*sn*-1, *sn*-2); glycerol methines (C1,3; C2); choline methyl [$N(CH_3)_3$]; choline methylenes ($N-CH_2$, $P-O-CH_2$); and terminal methyl (CH_3).

formation (Abei et al., 1993; Konikoff et al., 1994), and rhruematoid arthritis (Lazarevic et al., 1993). The existence of crystalline CHOL pools in oversaturated membranes has been suggested to stimulate antibody formation (Swartz et al., 1988).

In this work, we have performed a detailed multinuclear (^1H, ^{13}C, ^{31}P) MASNMR study of the DPPC/CHOL binary system with a large range of CHOL content (0−65 mol %) at temperatures below and above the main transition temperature of hydrated pure DPPC. We have analyzed ^{13}C chemical shifts, ^{13}C and ^{31}P line shapes, and ^1H and ^{31}P chemical shift anisotropy to obtain information about the molecular mobility and phase behavior of CHOL and DPPC. Particularly interesting results from this study include the following: (1) the chemical shifts of both *sn*-1 and *sn*-2 carbonyls were significantly affected by the incorporation of cholesterol; (2) chemical shift changes were observed for CHOL carbons as a function of mixing ratio; (3) crystalline monohydrated cholesterol was observed directly in a binary system with CHOL > 50 mol %; (4) crystalline CHOL affected the ^{31}P powder pattern under certain conditions of sample preparation.

MATERIALS AND METHODS

Materials. CHOL (>99% pure) was purchased from Nu-chek (Elysian, MN) and DPPC (>99% pure) from Avanti (Alabaster, AL). Both lipids were used as received. The purity of each sample was checked by TLC before and after NMR experiments, and no significant impurity contents were found.

Sample Preparation. Desired amounts of DPPC and CHOL were weighed into test tubes, dissolved in chloroform, and dried under a stream of N_2 gas to form a thin film around the bottom of the test tube, followed by vacuum drying overnight. The dry lipid thin films were hydrated in degassed D_2O (70 wt %). Because hydration is slow and inhomogeneous below the DPPC gel−liquid-crystalline transition of 41 °C, all lipid dispersions (unless otherwise noted) were warmed to 45 °C for 5 min with continuous sonication (bath) to accelerate hydration. The lipid dispersions were subjected to freeze−thaw cycles from −20 °C to 45 °C 5 times and stored at 4 °C before use. The compositions are expressed as mol % CHOL with respect to total lipid.

NMR Spectroscopy. All experiments were performed on a Bruker (Billerica, MA) AMX300 NMR spectrometer (7.05 T) equipped with solid-state accessories. Samples were loaded into 7 mm Zirconia rotors. A spherical Kel-F insert was used to cover the sample to prevent leakage and promote spinning. Total sample size was about 100 μL, with about 30−50 mg of dry lipids. The sample spinning rate was 4 kHz for all the MASNMR experiments, and 0 for the static NMR experiments. The chemical shifts were referred to the external reference standards: glycine carbonyl carbon for ^{13}C (176.06 ppm), phosphoric acid for ^{31}P (0 ppm), and tetramethylsiliane (0 ppm) for ^1H.

Differential scanning calorimetry (DSC) experiments were carried out with a Perkin-Elmer DSC-7 instrument (Norwalk, CT). Samples (20 μL) were sealed in a stainless-steel pan. An empty pan filled with 20 μL of D_2O was used as a reference. Heating and cooling rates were 5 °C/min. The instrument was calibrated by using the data obtained for a high-purity standard material (indium).

Optical microscopy experiments were performed on a Leitz-Dialux microscope fitted with a polarizer and heating stage 80 (Leitz/Wild, Burlington, MA).

RESULTS

General Features of ^{13}C MASNMR Resonances. Fully hydrated DPPC dispersions exist in the L_β' phase near ambient temperature, and undergo $L_\beta'-P_\beta'-L_\alpha$ phase transitions at 38 and 41 °C, respectively (Albon & Sturtevant, 1978). ^{13}C MASNMR spectra of DPPC are shown in Figure 1 for comparison with spectra of DPPC/CHOL mixtures. These spectra are similar to those obtained by other investigators (Forbes et al., 1988a,b; Wu & Chi, 1990), and revealed a characteristic spectrum for each phase. Briefly, the gel phase was represented by broad signals of the C=O, the internal methylene, $(CH_2)_n$, and the glycerol carbons as

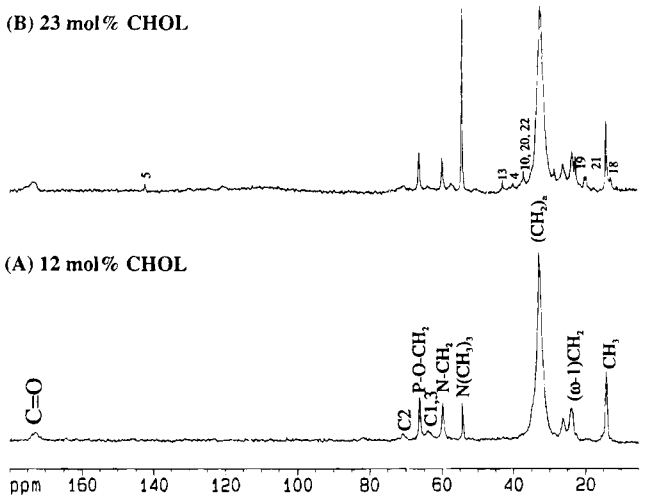

FIGURE 2: Proton-decoupled ^{13}C MASNMR spectra of fully hydrated DPPC/CHOL multilayers at 25 °C with (A) 12 mol % CHOL and (B) 23 mol % CHOL. Selected resonances are labeled for DPPC as Figure 1; peaks for CHOL are identified by standard numbering. All spectra were processed with 10 Hz line broadening; other conditions are the same as those in Figure 1.

a result of intermediate molecular motions [which interfere with the dipolar decoupling field (Oldfield et al., 1991)]. From L_{β}' to P_{β}', there was further line broadening because different conformations coexist and interchange in the P_{β}' phase (Wittebort et al., 1981; Wu & Chi, 1990). Above the main transition temperature (T_m), the L_{α} phase showed narrower resonances, and additional peaks [e.g., $CH_2C{=}O$, $(\omega\text{-}1)CH_2$] were resolved. Notably, the *sn*-1 and *sn*-2 C=O peaks were resolved into two peaks, and were assigned based on data from selectively [^{13}C]carbonyl-labeled DPPC (Schmidt et al., 1977). In addition, upon chain melting a large upfield shift of the $(CH_2)_n$ peak was observed, which reflects an increase in the population of gauche conformations (Vander-Hart, 1981).

When CHOL is incorporated into DPPC multilayers, the phase behavior of DPPC changes with the CHOL content, and these changes are reflected in the ^{13}C MASNMR spectral features. The P_{β}' phase is abolished at low CHOL content (McMullen et al., 1993). In the gel phase with low CHOL content, the ^{13}C MASNMR spectra were similar to that of pure DPPC (Figure 1A), except that the C=O peak became broader and asymmetric (see below), and the line shape of the $(CH_2)_n$ signal changed, becoming narrower at the peak but remaining broad near the base line (Figure 2A). CHOL signals became visible at about 23 mol % CHOL (Figure 2B), appearing as narrow peaks overlapping the broad signals of DPPC. This implies that the CHOL and the DPPC in close association with CHOL existed in a mobile liquid-crystal-like state, whereas DPPC not in close association with CHOL existed in a gel state. This observation is in agreement with the prediction that a disordered solid (S_o) phase and an ordered liquid-crystalline (L_o) phase coexist in DPPC multilayers with 10−30 mol % CHOL below T_m (Sankaram & Thompson, 1991; Vist & Davis, 1990). At higher CHOL content (>35 mol %), signals from the S_o phase were no longer detectable, and the ^{13}C resonances showed line widths characteristic of the liquid-crystalline DPPC/CHOL multilayers, indicating that the gel phase is abolished (spectrum not shown).

Figure 3 shows the ^{13}C MASNMR spectra of the DPPC/CHOL multilayers above T_m (45 °C) at selected CHOL contents. A spectrum of DPPC with 5 mol % CHOL (Figure 3A) was very similar to that of pure DPPC in the L_{α} phase, except for some small line narrowing, and slight chemical shift changes for the *sn*-1 C=O and $(CH_2)_n$ peaks (see below). The line narrowing may be caused by the reduction of chain−chain interactions between the hydrocarbon chains of DPPC in the presence of the small amount of CHOL. Above 10 mol %, the CHOL signals became readily detectable (Figure 3B). In all spectra of mixtures with <50 mol % CHOL, peaks for both CHOL and DPPC were narrow, and only one peak was observed for each carbon (Figure 3A−C), suggesting that stable CHOL-rich pools do not exist on the ^{13}C NMR time scale. This contrasts with a

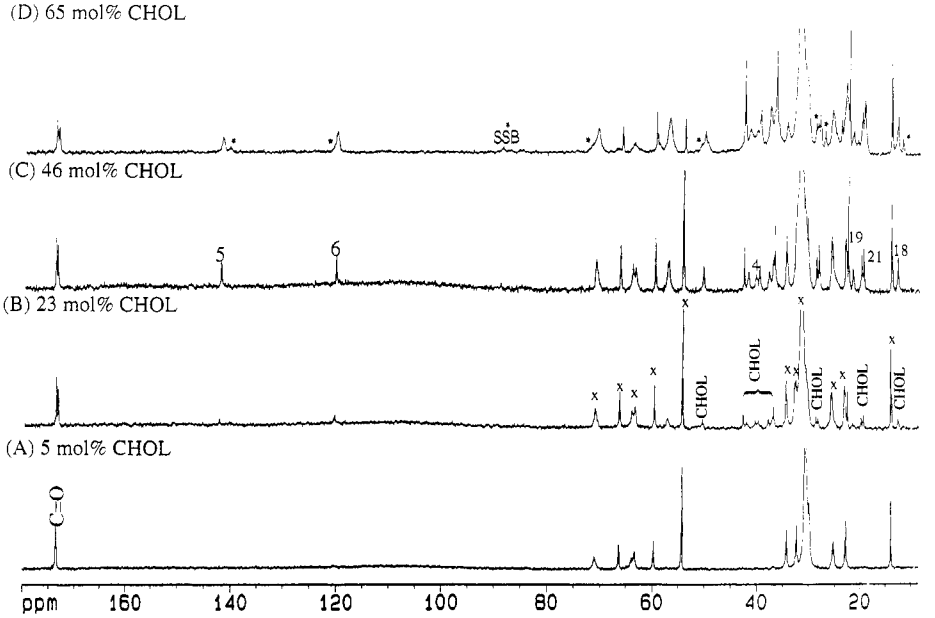

FIGURE 3: Proton-decoupled ^{13}C MASNMR spectra of fully hydrated DPPC/CHOL multilayers at 45 °C with (A) 5 mol % CHOL, (B) 23 mol % CHOL, (C) 46 mol % CHOL, and (D) 65 mol % CHOL. Selected CHOL signals are indicated by CHOL or by "x" for DPPC. Conditions for obtaining NMR spectra are the same as those in Figure 1.

report that ^{13}C-4 enriched CHOL yielded a second narrow signal above 20 mol % cholesterol in DPPC with static solid-state NMR (Opella et al., 1976). Although the C-4 region in the natural-abundance spectrum (Figure 3) is somewhat crowded, we did not observe a second resonance for other clearly resolved CHOL resonances until the formation of crystalline CHOL. Moreover, in a sample with 40 mol % ^{13}C-4-enriched CHOL in DPPC, we observed only one C-4 resonance.

Above 50 mol % CHOL, signals for both DPPC and CHOL became slightly broader, and several new CHOL resonances were observed (Figure 3D). The observation of a second set of narrow signals for CHOL indicates a second pool of CHOL in slow exchange with the CHOL pool observed at lower CHOL content. The new CHOL signals were attributed to crystalline CHOL monohydrate by comparison of the chemical shifts in Figure 3D with those of pure crystalline forms of anhydrous and monohydrate CHOL (Guo and Hamilton, unpublished results). We were not able to identify crystalline CHOL by DSC and optical microscopy in this sample (see below).

It is generally believed that the equilibrium maximum mixing ratio is one molecule of CHOL per molecule of phospholipid (Philips, 1990). However, this ratio was obtained by extrapolation in a eggPC−CHOL−water ternary phase diagram (Bourges et al., 1967). Metastable unilamellar vesicles can be prepared up to a mole ratio of 4 CHOL:1 DPPC by sonication; upon storage, CHOL is slowly released as CHOL monohydrate as seen by electron microscopy and DSC (Collins & Phillips, 1982). Small unilamellar PC vesicles containing more than an equimolar amount of CHOL can be stable for several months (Collins & Phillips, 1982). It is not clear whether there were submicrocrystalline aggregates in these vesicles, or whether similar mixing ratios can be achieved in multilayers.

Recently, the existence of a solid, slowly exchanging CHOL pool, in addition to the bilayer-incorporated liquid-crystalline CHOL pool, was reported in *Acholeplasma laidlawii* strain B membrane enriched with exogenous cholesterol to 29−41 mol % with respect to total lipids (Monck et al., 1993). The solid pool disappeared and merged with the bilayer pool after incubation at elevated temperature and/or after lyophilization and resuspension of the intact membranes (Monck et al., 1993). As the authors pointed out, the structure of this solid pool could not be established because of the lack of appropriate experimental methods. Particularly, X-ray diffraction was not able to detect the structure. The direct and simultaneous observation of crystalline CHOL and bilayer-incorporated CHOL by ^{13}C MASNMR may permit a noninvasive and definitive identification of crystalline CHOL in membranes such as the *A. laidlawii* membranes, in cultured foam cells (Tangirala et al., 1994), which are models of atherosclerosis, or in other biological samples.

Effect of CHOL on the Chemical Shifts of DPPC Carbonyl Carbons. To provide a more complete analysis of how CHOL influences the carbonyl regions of DPPC, the DPPC carbonyl signal(s) was (were) monitored by MASNMR as a function of CHOL content and temperature. Below the main transition temperature, such influences can be evaluated by the carbonyl line widths (Figure 4). At low CHOL content, the single carbonyl signal was broadened compared to pure DPPC, evidence of the S_o phase (Figure 4, ≤12 mol %

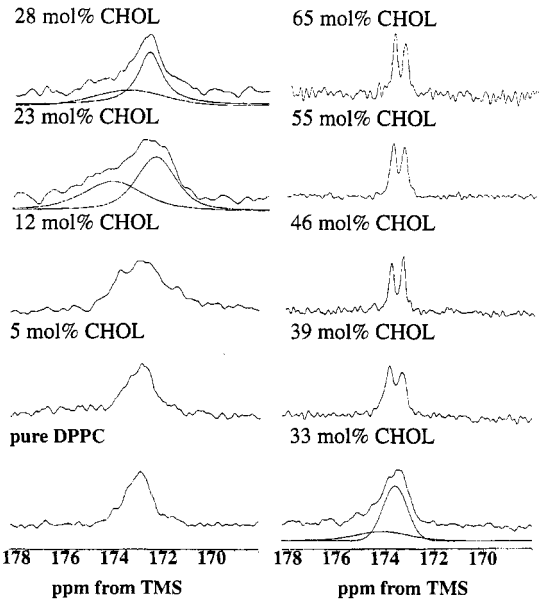

FIGURE 4: Carbonyl carbon signals of the DPPC/CHOL multilayers at 25 °C with varying CHOL content as indicated. Below 33 mol % CHOL, spectra were obtained with CPMAS and processed with 15 Hz line broadening; above this ratio, spectra were obtained without cross-polarization transfer and processed with 3 Hz line broadening. Selective signal deconvolutions were performed with Bruker deconvolution software. Other conditions are the same as those in Figure 1.

CHOL). With intermediate CHOL contents, the carbonyl peak became asymmetric and could be deconvoluted into two individual peaks (Figure 4, 12−33 mol % CHOL). The narrow component likely represents the L_o phase and the broad component the S_o phase. A similar observation of asymmetric carbonyl signals has been reported in a static solid-state ^{13}C NMR study (Huang et al., 1993). In the mixture of S_o+L_o, signals from the L_o phase are broader than those from individual L_o or L_α phases because the exchange rates between the L_o and S_o components are in the intermediate exchange rate regime of the ^{13}C NMR experiment (Huang et al., 1993). With higher CHOL contents, the S_o phase disappeared, and spectra revealed only the L_o phase, for which *sn*-1 and *sn*-2 carbonyls were resolved individually as narrow peaks (Figure 4, >33 mol % CHOL).

Above T_m, the DPPC/CHOL multilayers exist in the liquid-crystalline state. As shown in Figure 3, at 45 °C, the *sn*-1 and *sn*-2 carbonyl peaks of DPPC were resolved with a chemical shift difference ($\Delta\delta$) that was dependent on the CHOL content. At higher temperatures, the line width of the carbonyl carbons increased slightly, and the two peaks were not always resolved.

Figure 5A shows plots of the chemical shift values of the *sn*-1 (δ_1) and *sn*-2 (δ_2) carbonyls vs CHOL content at 45 and 55 °C. At 45 °C, δ_1 shifted upfield upon incorporation of small amounts of CHOL, whereas δ_2 was not affected. This argues against any strong H-bonding of CHOL with the *sn*-2 carbonyl in the mixture with <25 mol % CHOL. δ_1 continued to shift upfield and reached a minimum value at about 25 mol % CHOL and then shifted downfield. At approximately the same CHOL content, δ_2 shifted downfield in a manner similar to δ_1 until 50 mol % CHOL was reached, after which both chemical shifts remained constant.

Trends similar to those described for 45 °C were seen at 55 °C, except that at low CHOL content (<12 mol %), the

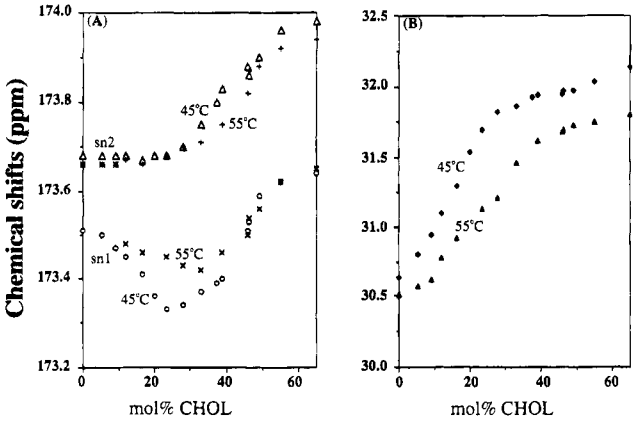

FIGURE 5: ^{13}C chemical shift of the carbonyl carbon (A) and acyl chain methylene carbon (B) of DPPC molecules as a function of CHOL content in the liquid-crystalline phase. The symbols are as follows: (△) *sn*-2 at 45 °C; (+) *sn*-2 at 55 °C; (○) *sn*-1 at 45 °C; (×) *sn*-1 at 55 °C; (♦) $(CH_2)_n$ at 45 °C; (▲) $(CH_2)_n$ at 55 °C. Symbols (+) and (×) overlap when the CHOL content is <12 mol % because the two peaks for *sn*-1 and *sn*-2 carbonyls were not resolved at 55 °C below this mixing ratio.

sn-1 and *sn*-2 carbonyls were not resolved. However, it is clear that δ_1 shifted upfield above 10 mol % CHOL and reached a minimum at about 30 mol % CHOL, whereas δ_2 began to shift upfield at about 25 mol % CHOL. At high CHOL content, δ_2 and δ_1 had values similar to those at 45 °C. The origin of the changes in δ_1 and δ_2 is not clear, but they showed the largest variation in the mixing ratio region where liquid-crystalline phase separation (L_d+L_o, L_d stands for disordered liquid-crystalline phase with low CHOL content) was predicted (Vist & Davis, 1990). Therefore, it is possible that in the L_d phase, the interactions of CHOL with DPPC cause an upfield shift of δ_1 and a downfield shift of δ_2 . In the L_o phase, a downfield shift was observed for both δ_1 and δ_2. If this assumption is correct, the interaction between DPPC/CHOL must be significantly different in the L_d and L_o phases, at least in the molecular segments near the carbonyl carbons.

In a recent study, Le Guerneve and Auger (1995) reported the observation of two carbonyl signals for dimyristoylphosphatidylcholine (DMPC) in the presence of 30 mol % CHOL at 30 °C in the liquid-crystalline multibilayer dispersion. They attributed the low-frequency peak to *sn*-1 and *sn*-2 carbonyl groups H-bonded to the hydroxyl group of the CHOL molecule, and the upfield peak to carbonyls that were not H-bonded to CHOL. We consider this interpretation to be unlikely for the following reasons: (1) the chemically different *sn*-1 and *sn*-2 carbons appear as two peaks in the ^{13}C MASNMR spectrum of pure DPPC, and the addition of CHOL increases the separation between the two peaks (Figure 3); (2) the two carbonyls of DMPC in multilayer dispersions have different CSA's in the absence of CHOL, and the addition of cholesterol significantly affects the CSA of the *sn*-1 carbon but has essentially no effect on the *sn*-2 carbonyl (Cornell & Keniry, 1983); (3) a previous MASNMR study of DPPC with a ^{13}C-enriched *sn*-2 carbonyl showed only one peak, with or without CHOL (Sankaram & Thompson, 1991); (4) the CHOL and PC molecules in mixed bilayers can move rapidly in the plane of the liquid-crystalline bilayer, with similar lateral diffusion coefficients ($\sim 10^{-8}$ cm^2 s^{-1}; Phillips, 1990). With such a high lateral diffusion rate, it seems unlikely to have a stable H-bonding

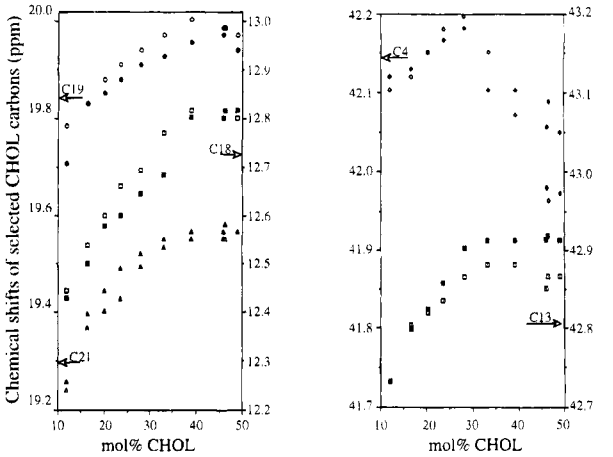

FIGURE 6: ^{13}C chemical shifts of selected CHOL carbons in DPPC/CHOL multilayers as a function of CHOL content at 45 °C (open symbols) and 55 °C (closed symbols). The symbols are (△) C21, (○) C19, (□) C18, (◇) C4, and (⊡) C13.

with a mean lifetime longer than 37 s, corresponding to the reported 0.5 ppm separation on a 7.05 T NMR instrument (Le Guerneve & Auger, 1995).

Effect of CHOL on the Chemical Shift of the Acyl Chains of DPPC. The ^{13}C MASNMR spectra showed significant changes in the center position of the envelope of resonances representing the internal methylenes of the DPPC acyl chains. Figure 5B shows the plots of the chemical shift of the $(CH_2)_n$ peak (δ_n) as a function of CHOL content. At 45 °C, δ_n shifted downfield almost linearly with increasing CHOL content, but with a larger slope at lower CHOL content. The two segments of the curve intersected at 30 mol % CHOL. At 55 °C, the slope was smaller in the low CHOL content region but remained similar to that at 45 °C in the high CHOL region, and the two segments intersected at about 40 mol % CHOL. The mixing ratios of 30 and 40 mol % CHOL lie on the phase separation boundary between two different liquid-crystalline phases [(L_o+L_d) and L_o] in the diagram at 45 and 55 °C, respectively (Huang et al., 1993). Therefore, the chemical shift changes of the $(CH_2)_n$ peak displayed in Figure 5B could be interpreted as indirect evidence for the phase separation above T_m. The downfield shift results from the increase of population of the trans-conformation of DPPC acyl methylenes caused by the incorporation of CHOL (Huang et al., 1993).

Chemical Shifts of CHOL Carbons in the Liquid-Crystalline Phase. Figure 6 shows the dependence of the chemical shift of selected CHOL carbon resonances (e.g., C13, C18, C19, C21, C4) on the mixing ratio at 45 and 55 °C. These resonances are well resolved, and are more sensitive to the mixing ratio. (Other carbons such as C5 and C6 were well resolved but showed no significant dependence on the mixing ratio; although the C3 carbon is presumably sensitive, it is superimposed on the glycerol carbon.) The chemical shifts for C13, C21, C18, and C19 followed a similar pattern, with a minor dependence on temperature. With increasing CHOL content, the chemical shifts first moved downfield, and then leveled off at 30−40 mol % CHOL. In contrast, the C4 resonance showed a distinctly different pattern, first shifting downfield slightly and then upfield almost linearly. The transition point was about 30 mol % CHOL.

Engleman and Rothman (1972) predicted that at ≤33 mol % CHOL, each CHOL molecule will be surrounded by seven

acyl chains of phospholipid molecules in its nearest environment; above this ratio, direct contacts between CHOL molecules are formed. As shown in Figure 6, the chemical shifts changes were significant below (but not above) this ratio, except for C4. This implies that the increasing orientational order in DPPC multilayers (caused by CHOL incorporation) progressively reduced the shielding on the carbons of CHOL that can make particularly close contacts with the DPPC acyl chains, such as C18, C19, and C21. (C13 is not directly in contact, but is affected by the adjacent C19; thus, it has a smaller chemical shift change). Above 30–40 mol % CHOL, the chain-disordered DPPC molecules (with acyl chains not in direct contact with CHOL) were no longer present, and further increases in CHOL content did not cause significant changes in the chemical shifts of these CHOL angular methyl carbons.

The chemical shift of the C4 resonance of CHOL showed a unique behavior, because the shielding on C4 is affected by two opposing effects. First, the incorporation of CHOL increased the acyl chain order of DPPC, leading to a deshielding effect on the CHOL C4 carbon (as on other CHOL carbons described above). Second, increased exposure of the CHOL hydroxyl to the polar interfacial region results in an upfield shift of the C4 carbon (Lund-Katz & Phillips, 1981). At low CHOL content, the first effect was slightly larger than the second, and the net effect was a small downfield shifting. Above 29 mol % CHOL, the C4 shift began to move upfield as the second effect dominated. Recently, Sankaram and Thompson (1990) suggested that at low CHOL content, a CHOL molecule lies in the nonpolar center of a bilayer and extends into both layers. At higher CHOL content (>25–33 mol %), CHOL is anchored in the bilayer interfacial region through H-bonding between its hydroxyl group and the *sn*-2 carbonyl. Although our results do not necessarily support the hypothesis of specific H-bonding, the C4 chemical shift change (Figure 6) is consistent with the displacement of the CHOL hydroxyl group from a more nonpolar region (the bilayer core) to a more polar region (the interfacial region).

Apparent Chemical Shift Anisotropy of the Acyl Chain Protons in the Liquid-Crystalline Phase as a Function of CHOL Content. In the liquid-crystalline phase, almost all expected signals from DPPC were resolved in the ^{1}H MASNMR spectra of DPPC and DPPC/CHOL multilayers (Figure 7A), and the intense $(CH_2)_n$ peak was flanked by its spinning sidebands as reported previously (Forbes et al., 1988a,b). Signals from the sterol protons were not detected, consistent with the results of Forbes et al., (1988b).

Although the acyl chain protons are most directly affected by the incorporation of CHOL, little information about CHOL–DPPC interactions is obtained if only the isotropic chemical shift is considered, since homonuclear coupling causes the $(CH_2)_n$ peak to be broad. Another important physical property that is sensitive to intermolecular interaction is the chemical shift anisotropy, which is not seen directly with the MASNMR spectrum, but is preserved in the spinning sidebands (ssb) of the $(CH_2)_n$ peak. From the intensity distribution of the ssb, the apparent chemical shift anisotropy ($\Delta\sigma$) can be calculated for the $(CH_2)_n$ protons (Herzfeld & Berger, 1980). ^{1}H spectra were obtained as a function of CHOL content at 45 °C for the calculation of $\Delta\sigma$. As shown in Figure 7B, $\Delta\sigma$ first increased with CHOL content and then leveled off at >30 mol % CHOL. The

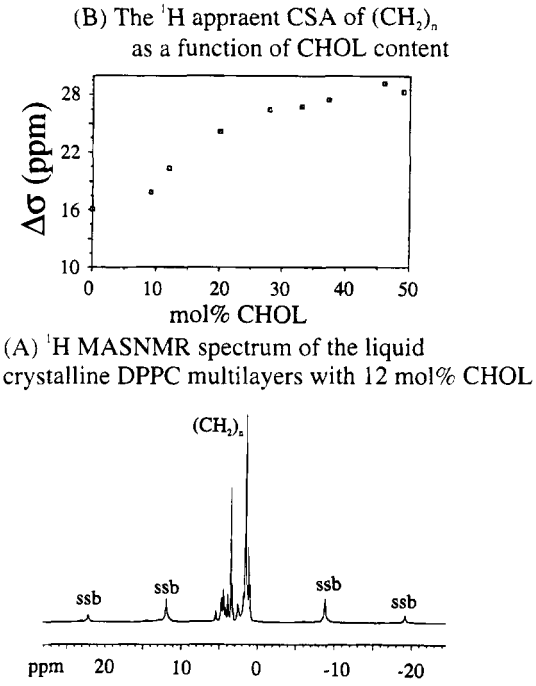

FIGURE 7: (A) ^{1}H standard single-pulse MASNMR spectrum of DPPC with 12 mol % CHOL at 45 °C; the acyl chain methylene proton signal [$(CH_2)_n$] flanked with its spinning sidebands (ssb) is indicated. (B) Apparant chemical shift anisotropy of the methylene protons as a function of CHOL content.

increase in $\Delta\sigma$ reflects the increasing order of the acyl chains as CHOL is incorporated into the DPPC bilayer and corresponds well with the ^{13}C chemical shift changes of the $(CH_2)_n$ signal (Figure 5B). The agreement between the ^{1}H and ^{13}C NMR data also indicates that the contribution from the CHOL signals to the calculated $\Delta\sigma$ is negligible.

^{31}P Static Solid-State NMR and MASNMR. ^{31}P NMR spectroscopy was used to obtain information about the aqueous polar region of DPPC with different CHOL contents. Figure 8 shows the powder pattern of ^{31}P NMR spectra in the DPPC/CHOL binary system at varying mixing ratios (<50 mol % CHOL), at temperatures below (25 °C) and above (45 °C) T_m. All the spectra show an axially symmetric powder pattern as a result of motional averaging. Spectra obtained at 55 °C were not significantly different (not shown). The values of chemical shift anisotropy ($\Delta\sigma$; Table 1) were measured as the spectral width. For pure DPPC below T_m, the line shape was broad because of the slow motions in the gel phase. Above T_m, the expected line shape and $\Delta\sigma$ value (~46 ppm; Li et at., 1993) were observed.

The addition of CHOL affected the ^{31}P line shape differently below and above T_m. Below T_m, there was a gradual narrowing with increasing CHOL, and the signal at $\sigma_\perp$ became sharp, reflecting the presence of the liquid-crystalline phase in coexistence with the gel phase. At >23 mol % CHOL, the spectral feature of the liquid-crystalline phase dominated. These ^{31}P line shape changes show a gradual abolishment of the gel phase by CHOL, consistent with the ^{13}C MASNMR data of Figure 4.

Figure 9 gives the corresponding ^{31}P MASNMR spectra of samples studied in Figure 8 at 25 °C. A moderate amount of CHOL (Figure 9C,D) severely broadened the MAS signals, reflecting the intermediate exchange between the S_o and L_o phases. The broad line width persisted up to the mixing ratio of about 35 mol % (not shown), and then the

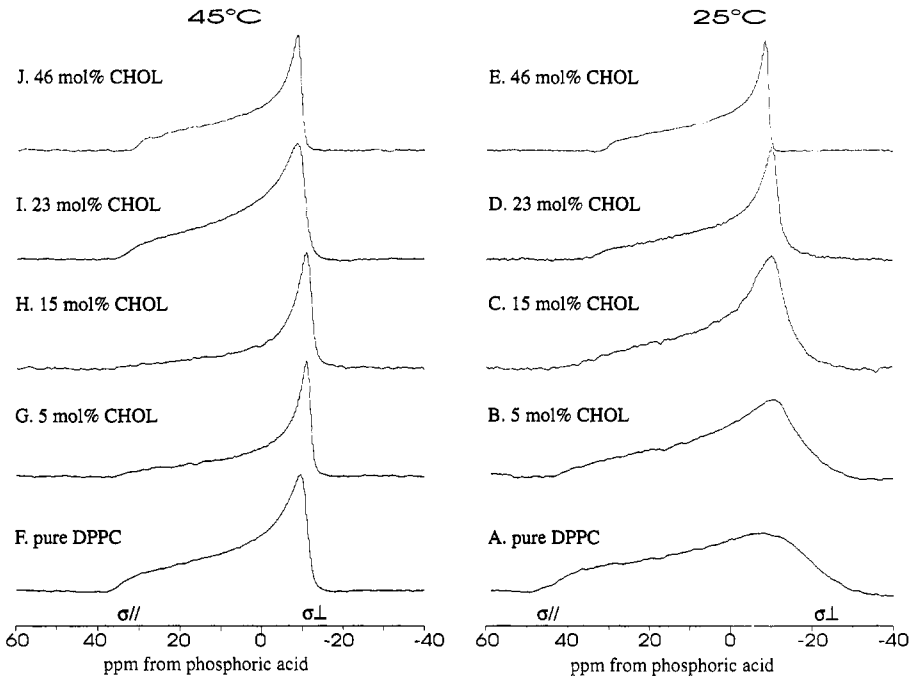

FIGURE 8: Static ^{31}P NMR spectra of DPPC with varying CHOL content at 25 °C (right column) and 45 °C (left column). All spectra were obtained with a standard single-pulse experiment with high-power proton decoupling, with 4K data points zero-filled to 8K, and processed with 15 Hz line broadening. The CHOL contents are labeled with the corresponding spectra, and the symbol $\sigma_\perp$ represents the abundant edge of the chemical shift distribution.

Table 1: ^{31}P CSA Values (±1 ppm) of DPPC at Various CHOL Contents and Temperatures

temp (°C)	pure DPPC	5 mol %	15 mol %	23 mol %	46 mol %	65 mol %
25	67	58	50	46	41	35
45	47	46	48	47	41	34
55	44	46	46	43	41	35
62	44	46	46	43	41	32

signal became narrow again as the S_o disappeared. The phase boundary thus estimated is about the same as that from the ^{13}C MASNMR results (described above). It is important to note that with static NMR, the ^{31}P powder pattern for samples with 23 mol % and 46 mol % CHOL were rather similar; however, with MASNMR they were significantly different, reflecting the limitation of static ^{31}P NMR for phase identification below T_m.

Above T_m, the MASNMR ^{31}P spectra (not shown) were less informative since they all resembled that of a typical liquid-crystal phase (e.g., Figure 9E). On the other hand, the static spectra (Figure 8, left panel) of pure DPPC and DPPC/CHOL with ≥23 mol % CHOL were quite similar. In contrast, static ^{31}P spectra of DPPC with 5−15 mol % CHOL (Figure 8G,H) were significantly different from either pure DPPC (Figure 8F) or mixtures with higher CHOL content (Figure 8I,J). For these samples, the signal intensity distribution near the upfield edge ($\sigma_\perp$) component was much higher than a normal axially symmetric powder pattern, whereas the signal intensity at or near the downfield edge ($\sigma_{||}$) was very low. Since the mixing ratios of 5−15 mol % CHOL were predicted to have phase-separation above T_m (Vist & Davis, 1990), the abnormal features of the ^{31}P spectra (Figure 8G,H) might be caused by the chemical exchange between the coexisting phases.

Table 1 summarizes the $\Delta\sigma$ values of varying CHOL contents at different temperatures. There is a gradual

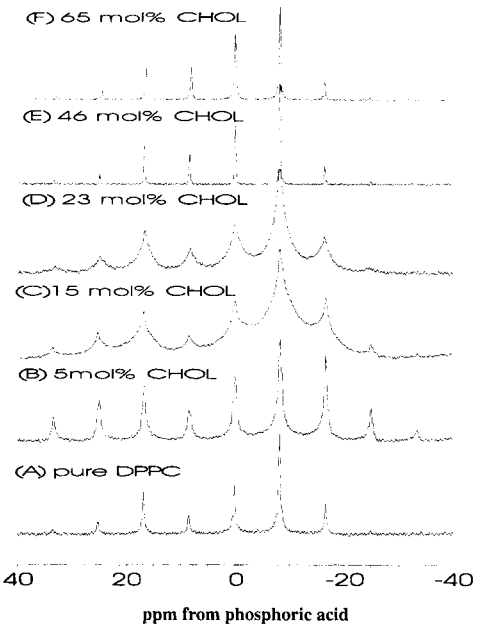

FIGURE 9: ^{31}P MASNMR spectra of DPPC with varying CHOL content at 25 °C. All spectra were obtained with a standard single-pulse experiment with high-power proton decoupling, 1 kHz MAS spinning rate, 4K data points zero-filled to 8K, and processed with 3 Hz line broadening. The CHOL contents are labeled with the corresponding spectra.

reduction in $\Delta\sigma$ as CHOL increases, in agreement with the early observation that CHOL reduces intermolecular headgroup interactions and increases the motional freedom of the phosphorylcholine moiety (Yeagle et al., 1977).

Since the ^{13}C MASNMR spectra showed clear evidence of CHOL crystals in DPPC with >50 mol % CHOL, we investigated the effect of CHOL crystallization on the DPPC headgroup. The ^{31}P powder pattern for 65 mol % CHOL showed an axially asymmetric line shape with the highest intensity at −2 ppm, slightly downfield from $\sigma_\perp$ at −10 ppm

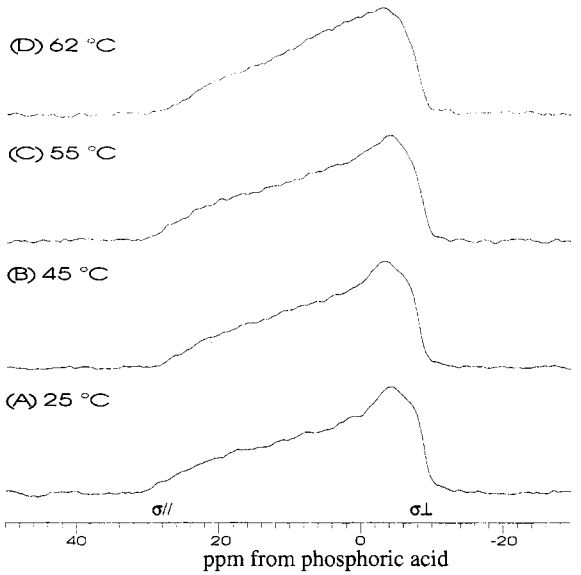

FIGURE 10: Static ^{31}P NMR spectra of DPPC with 65 mol % CHOL at different temperatures. All spectra were obtained as in Figure 8 and processed with 15 Hz line broadening. The experimental temperatures are labeled with the corresponding spectra, and the symbol $\sigma_\perp$ represents the abundant edge of the chemical shift distribution.

(Figure 10). The line width ($\Delta\sigma$) was smaller (34 ppm) than that for mixtures with <50 mol % CHOL (41−46 ppm), but the signal distribution in the middle region (between $\sigma_\perp$ and $\sigma_{||}$) was abnormally high. With increasing temperature, the narrow component at −2 ppm became less apparent, and the intensity in the middle increased. A similar line shape change in the ^{31}P powder pattern was observed in a DMPC/gramicidin A mixture and was explained by the microscopic sample heterogeneity caused by the polar group protein−lipid interactions and by polar group protein steric interactions (Rajan et al., 1981). In this work, the abnormal ^{31}P spectral features were observed only in samples with crystalline CHOL monohydrate detected by ^{13}C MASNMR, and might be indicative of submicrocrystals near the phosphorylcholine moiety.

In general, the addition of CHOL caused substantial changes in the ^{31}P powder pattern of DPPC, particularly at moderate mixing ratios and above the saturation limit (50 mol % CHOL). It was previously reported that the incorporation of up to 50 mol % CHOL into DPPC multilayers produced little change in ^{31}P chemical shielding anisotropies compared with pure DPPC (Brown & Seelig, 1978). However, this conclusion was based on studies with a more limited scope and specifically on samples with rather high CHOL content (>25 mol % CHOL) at a temperature well above T_m, 58 °C (Brown & Seelig, 1978). The abnormal line shapes of DPPC with moderate amounts of CHOL at 45 °C (Figure 8G,H) were therefore not seen in the prior study.

Identification of CHOL Monohydrate in DPPC/CHOL Multilayers by DSC and Optical Microscopy. Crystalline CHOL monohydrate is characterized by a platelike morphology under a polarizing microscope (Loomis et al., 1979). Pure CHOL monohydrate undergoes a phase transition to an anhydrous form at about 90 °C. To compare the applicability of these two methods with NMR methods for the identification of the CHOL monohydrate in the DPPC/CHOL multilayers, the following experiments were performed. First, a thin film of DPPC with 62 mol % CHOL was prepared by as described under Materials and Methods and hydrated with 70 wt % D_2O at 45 °C, except that bath sonication was replaced by votexing for 10 min, and the freeze−thaw cycles were omitted. Aliquots of the lipid dispersion were loaded at the same time into a DSC pan, on an NMR rotor, and onto a microscope glass slide. By polarizing microscopy, large (~μm) platelike crystals featuring CHOL monohydrate were observed outside the Maltese crosses of lipid multilayers. The characteristic phase transition at about 90 °C was also observed in the DSC trace. The ^{13}C MASNMR spectrum clearly showed the signals from CHOL monohydrate, as in Figure 3D. However, the ^{31}P static NMR spectrum at 25 °C (not shown) was similar to the normal pattern, such as that for the sample with 46 mol % CHOL (Figure 8J). Therefore, without sonication and freeze−thaw treatment, large CHOL monohydrate crystals can be detected by DSC and optical microscopy in addition to ^{13}C MASNMR. Because these large crystals were located outside of the membrane structure, they did not affect the static ^{31}P spectrum.

Following these experiments, an aliquot of the same lipid dispersion was bath-sonicated at 45 °C for 5 min, and then passed through a freeze−thaw cycle 5 times as for the other samples. The same protocols were repeated for the detection of crystals. The ^{13}C MASNMR spectrum was the same as before the sonication, and revealed crystalline CHOL monohydrate (Figure 3D). In contrast, the phase transition observed by DSC at 90 °C became very diffusively broad, and crystals were not visible under the polarizing microscope. Moreover, the static ^{31}P spectrum showed the "abnormal" feature as in Figure 10.

DISCUSSION

The molecular details of the interactions of cholesterol with phospholipids in bilayers have been the subject of numerous experimental and theoretical studies. A key point of interaction could be the hydrogen-donating group, the 3β-hydroxyl of CHOL, which can in principle form a H-bond with a suitable acceptor, such as the ester oxygens of phospholipids (Fong et al., 1977; Brockerhoff et al., 1974; Keough et al., 1973). H-bonding has been suggested to occur between the CHOL hydroxyl and either the *sn*-1 (Huang, 1977) or the *sn*-2 (Presti et al., 1982; Boggs, 1987) carbonyl carbons, or even the phosphate group (Darke et al., 1972; Robinson et al., 1995). H-bonding between the CHOL hydroxyl and the phosphate group has been shown to be unlikely since the latter binds to water more strongly (Yeagle & Martin, 1976; Yeagle et al., 1975; Wong et al., 1989). H-bonding of the CHOL hydroxyl to the *sn*-1 carbonyl has also been generally refuted by a variety of investigations (Siminovitch et al., 1987; Levin et al., 1985; Wong et al., 1989).

H-bonding in anhydrous DPPC containing 20 mol % anhydrous CHOL was evidenced by the stretching frequency shifts of the *sn*-2 (but not the *sn*-1) carbonyl (Wong et al., 1989). Such shifts were found to be larger than the corresponding shifts caused by the hydration of the *sn*-2 carbonyl, implying the H-bonding between the CHOL hydroxyl and *sn*-2 carbonyl is stronger than that between free water and the *sn*-2 carbonyl, and the authors thus argued that water molecules cannot replace the CHOL hydroxyl as the H-bond donor even in an excess of water (Wong et al.,

1989). However, this argument was based on the assumption that the CHOL hydroxyl would not interact with water but only with the *sn*-2 carbonyl (Wong et al., 1989). Since all CHOL molecules are hydrated either as monomers or as monohydrated crystals as evidenced by the ^{13}C MASNMR (Figure 3), the H-bond between the *sn*-2 carbonyl and the CHOL hydroxyl in the anhydrous mixture could be possibly replaced by H-bonds with water molecules.

Other plausible evidence for the H-bonding of the CHOL hydroxyl to the *sn*-2 carbonyl includes the observed downfield shifts of the *sn*-2 ^{13}C carbonyl resonance in DPPC multilayers containing 50 mol % CHOL (Sankaram & Thompson, 1991). However, this observation was made on DPPC with ^{13}C labeling at the *sn*-2 carbonyl, and information from the *sn*-1 carbonyl was obscured.

On the other hand, many studies have suggested the nonexistence of H-bonding between the CHOL hydroxyl and the ester carbonyl groups, including Raman and infrared spectroscopy (Bush et al., 1980; Clejan et al., 1979), ^{2}H NMR studies of the ^{2}H-labeled CHOL C3 carbon (Higinbotham et al., 1993), and a study of the rate of lipid desorption from membranes (Slater et al., 1993). In addition, it was reported that the chemical shifts and the relaxation times of the ^{13}C-labeled CHOL C4 carbon were the same in the hydrated bilayers of diester and diether phosphatidylcholines containing 10 mol % CHOL, and there were no specific requirements for ester or ether linkages in phosphatidylcholine for CHOL to reduce bilayer permeability (Bittman et al., 1984). Since the ether oxygen is a weaker H-bond acceptor than the ester oxygen, the indistinguishable chemical shieldings on the CHOL C4 carbon suggest that the specific H-bondings between the CHOL hydroxyl and the ester carbonyls are not likely.

It was also reported that as a cholesterol analog, 3-doxyl-5α-cholestane interacts very weakly with phospholipid bilayers, which was attributed to the inability of this analog to form a H-bond with the carbonyl groups of the acyl chains of phospholipid because of the lack of a H-bond donor (Somjen et al., 1995). However, this may be due to the lack of the C5−C6 double bond, which has been shown to be a most critical requirement for optimal sterol−phospholipid interactions (Ranadive & Lala, 1987). Consistent with the latter interpretation are observations that the methyl ether of cholesterol (also lacking an H-bond donor) was found to be equally compatible both in artificial and in natural membranes (Lala et al., 1979; Demel et al., 1984). More recently, a hydrophobic mismatching hypothesis was proposed based on the observation that the interaction between sterol and phospholipids was dependent on the length of both the acyl chain and the C17 side chain (McMullen et al., 1993, 1994, 1995). For example, androstenol, which has the same structure as cholesterol except it lacks the C17 isooctyl side chain, was found to be much less effective than cholesterol in ordering the liquid-crystalline bilayers of DPPC (Senak et al., 1992; McMullen et al., 1994). These reported observations also show that H-bonding is not essential to account for the sterol−phospholipid interactions.

Our ^{13}C MASNMR study showed that both the carbonyls and the acyl chain methylenes are significantly affected by the incorporation of CHOL, indicating strong interactions in both the polar and nonpolar regions of DPPC/CHOL multilayers. The acyl chain ordering effect caused by DPPC/CHOL hydrophobic interactions is well evidenced by the change in the chemical shifts of the methylene carbons (Figure 5B) and the CSA of the methylene protons (Figure 7B). Assessing the effects of CHOL on the polar region of DPPC is less straightforward. As shown in Figure 5A, both *sn*-1 and *sn*-2 carbonyls (chemical shift and line shape) are affected by CHOL, and the *sn*-1 is affected more than the *sn*-2 at low CHOL content (<35 mol % CHOL, Figure 5A). However, these effects may not be due solely or primarily to H-bonding.

Early static ^{13}C NMR studies on the DMPC/CHOL liquid-crystalline dispersion with up to 37 mol % suggested that CHOL has little effect on the CSA of the *sn*-2 carbonyl, but caused a substantial increase in the CSA of the *sn*-1 carbon (Cornel & Keniry, 1983). In our DPPC/CHOL multilayers, the change in the *sn*-2 carbonyl chemical shift was insignificant up to 30 mol %. Because the *sn*-2 carbonyl group is very sensitive to local conformational changes, these results for both DMPC and DPPC may indicate that up to a certain critical mixing ratio (which is also dependent on the acyl chain length), there are no conformational changes in the vicinity of the *sn*-2 carbonyl region (Cornel & Keniry, 1983). Above these critical mixing ratios, the static NMR line width of the *sn*-2 carbonyl resonance of DPPC did not change (Huang et al., 1993), but the chemical shift changed significantly (Figure 5A, this work; Sankaram & Thompson, 1991).

The exact origin of these changes is not clear. To account for the increasing CSA of the *sn*-1 carbonyl with the addition of ≤37 mol % CHOL in DMPC, it was suggested that CHOL gradually eliminates the motion of the carbonyl group, leaving it approaching a simple rapid rotation about the bilayer normal in the liquid-crystalline dispersion (Cornel & Keniry, 1983). This explanation was based on the assumption that the isotropic chemical shift was unaffected by the addition of CHOL, which our results show to be reasonable because the isotropic chemical shift changes were relatively small (<0.2 ppm for DPPC, Figure 5A); in comparison, the CSA changed from 27 ppm for pure DMPC to about 50 ppm for DMPC with 37 mol % CHOL. Therefore, for the DPPC/CHOL mixture below the critical mixing ratio of ~30 mol % CHOL, the *sn*-1 carbonyl chemical shift changes might also be a result of restrictions of the acyl chain motions. This explanation is supported by recent ^{2}H NMR studies, which indicated that the incorporation of CHOL (11 mol %) in fully hydrated DMPC multilayers significantly increased the order parameter of the upper half of the *sn*-1 chain but did not affect the *sn*-2 chain (Robinson et al., 1995).

Above the mixing ratio of 30 mol % CHOL, the addition of CHOL causes downfield ^{13}C chemical shift changes of the *sn*-1 and *sn*-2 carbonyl in the same manner. This corresponded to the transition in the C4(CHOL) chemical shift changes (Figure 6), and might be a result of rearrangement of CHOL molecules in the bilayers which enables the polar end of CHOL be more exposed to the interfacial region. The fact that *sn*-1 and *sn*-2 carbonyl chemical shifts were affected in the same manner could indicate that instead of forming a specific H-bond with the *sn*-2 carbonyl (Sankaram & Thompson, 1991), the CHOL molecules interact more equally with both acyl chains [all the acyl chains are in direct contact with CHOL above this ratio (Hui, 1993)] and also undergo rapid interchange between all sites of close interaction. These chemical shift effects may also reflect the finding

that the location of the two carbonyls of DPPC in the interface may be more equivalent than previously thought (Smith et al., 1992; Wong et al., 1989).

Previous NMR, X-ray, and neutron-diffraction studies have shown that for pure phosphatidylcholine bilayers, the phosphorylcholine headgroup lies approximately parallel to the membrane surface (Worcester & Franks, 1976; Griffin et al., 1978; Seelig & Gally, 1976; Yeagle et al., 1977). Addition of CHOL increases the separation between the phospholipid headgroups, as shown by X-ray diffraction (Levine, 1972) and $^{31}P\{^1H\}$ NOE measurements (Yeagle et al., 1977). As a result, the phosphorylcholine moiety can experience increasing freedom of motion (MacLaughlin et al., 1975). Our results show a reduction of the ^{31}P spectral width ($\sigma_{\parallel} - \sigma_{\perp}$), consistent with increased motional freedom of the phosphate (Table 1).

Although phase separations in DPPC/CHOL mixtures have been widely described, the phase boundaries in the phase diagram have been controversial. Most phase diagrams in the literature are based on differential calorimetry data, which measure the chain melting temperature as the phase transition temperature. For two phases coexisting with one diminishing phase, the minor component could be well obscured by the major component when the bulk phase properties are measured. Our studies revealed a discrepancy with predictions of some published phase diagrams as to the phase boundary between the S_o and the S_o+L_o phases. For example, this has been denoted by a nearly vertical line at 20−25 mol % CHOL (Vist & Davis, 1990) or 25−30 mol % CHOL (Sankanram & Thompson, 1991). These phase boundaries would predict a liquid-crystal-like spectrum representative of the L_o phase as the sole feature of the ^{13}C spectrum for 25 mol % CHOL at 25 °C (below T_m). However, the S_o phase remained significant (coexisting with the L_o phase) in the ^{13}C MASNMR spectra until 35−40 mol % CHOL (Figure 4). Theoretical work on the DPPC/CHOL system (Scott, 1977) using the Monte Carlo simulation shows a phase diagram in which the line separating the S_o+L_o phase from the L_o phase is not vertical but slopes toward higher CHOL content, and the single phase (L_o) region starts at 40 mol % CHOL (Scott, 1977). This ratio is close to our observations, and is also in close agreement with the experimental phase diagram by Huang et al. (1993).

^{13}C MASNMR experiments with CHOL in a slight molar excess of DPPC revealed characteristic signals for the monohydrate crystal of CHOL. Optical microscopy and DSC were used in conjunction with ^{13}C MASNMR to monitor crystal formation under different conditions of sample preparation. From these experiments with CHOL in molar excess of DPPC, we found that (i) without sonication and freeze−thaw cycles, large CHOL monohydrate crystals formed outside the multibilayer but did not affect the static ^{31}P NMR lineshape; (ii) bath sonication and freeze-thaw cycles helped to break down the CHOL monohydrate crystals and increase the incorporation into the multibilayer; (iii) CHOL monohydrate crystals were detected by ^{13}C MASNMR in some samples which did not show crystals by DSC or optical microscopy; and (iv) submicroscopic crystals caused a significant change in the ^{31}P line shape, implying that they might be located near the phosphate groups.

These results suggest that in membranes that become oversaturated with CHOL, crystallization may begin around the headgroup region. This could affect membrane function and might also play a role in the mechanism for antibody formation to crystallized cholesterol in membranes (Swartz et al., 1988). Crystals formed in this manner, as opposed to crystallization outside the membrane in larger crystals, may be easier to dissolve and be reabsorbed into the membrane if the cholesterol/phospholipid ratio decreases. Our model systems allow testing of this hypothesis by a combination of multinuclear solid-state NMR with or without magic angle spinning. Such studies can provide a more detailed description of the molecular events in cholesterol crystallization and dissolution that is relevant to several diseases, most notably atherosclerosis.

REFERENCES

Abei, M., Schwarzendrube, J., Nuutinen, H., & Broughan, T. A. (1993) *J. Lipid Res. 34*, 1141−1148.

Albon, N., & Sturtevant, J. M. (1978) *Proc. Natl. Acad. Sci. U.S.A. 75*, 2258−2267.

Bittman, R., Clejan, S., Lund-Katz, S., & Phillips, M. C. (1984) *Biochim. Biophys. Acta 772*, 117−126.

Boggs, J. M. (1987) *Biochim. Biophys. Acta 906*, 353−404.

Bonmatin, J.-M., Smith, I. C. P., Jarrell, H. C., & Siminovitch, D. J. (1990) *J. Am. Chem. Soc. 112*, 1697−1704.

Bourges, M., Small, D. M., & Dervichian, D. G. (1967) *Biochim. Biophys. Acta 137*, 157−167.

Brainard, J. R., & Cordes, E. H. (1981) *Biochemistry 20*, 4607−4617.

Brockerhoff, H. (1974) *Lipids 9*, 645−650.

Brown, M. F., & Seelig, J. (1978) *Biochemistry 17*, 381−384.

Bush, S. F., Adams, R. G., & Levin, I. W. (1980a) *Biochemistry 19*, 4429−4436.

Bush, S. F., Adams, R. G., & Levin, L. W. (1980b) *Chem. Phys. Lipids 27*, 101−111.

Clejan, B., Bittman, R., Deroo, P. W., Isaacson, Y. A., & Rosenthal, A. F. (1979) *Biochemistry 18*, 2118−2125.

Collins, J. J., & Phillips, M. C. (1982) *J. Lipid Res. 23*, 291−298.

Cornell, B. A., & Keniry, M. (1983) *Biochim. Biophys. Acta 732*, 705−710.

Darke, A., Finer, E. G., Flook, A. G., & Phillips, M. C. (1972) *J. Biol. Chem. 63*, 265−279.

Demel, R. A., Lala, A. K., Nanda, K. S., & van Deenen, L. L. M. (1984) *Biochim. Biophys. Acta 771*, 142−150.

Engleman, D. M., & Rothman, J. E. (1972) *Nature 247*, 3694−3697.

Fong, J. W., Tirri, L. J., Deshmukh, D. S., & Brockerhoff, H. (1977) *Lipids 12*, 857−862.

Forbes, J., Husted, C., & Oldfield, E. (1988a) *J. Am. Chem. Soc. 110*, 1059−1065.

Forbes, J., Bower, J., Shan, X., Moran, L., & Oldfield, E. (1988b) *J. Chem. Soc., Faraday Trans. 1 84*, 3821−3849.

Frank, N. P. (1976) *J. Mol. Biol. 100*, 345−359.

Griffin, R. G., Powers, L., & Pershan, P. S. (1978) *Biochemistry 17*, 2718−2722.

Hamilton, K. S., Jarrell, H. C., Briere, K. M., & Grant, C. W. M. (1993) *Biochemistry 32*, 4022−4028.

Hammond, J. R. (1994) *J. Pharmacol. Exp. Ther. 271*, 906−917.

Herzfeld, J., & Berger, A. E. (1980) *J. Chem. Phys. 73*, 6021−6030.

Higinbotham, P. H., Beswick, R. J., Malcolmson, D. R., Parkinson, J. A., & Sadler, I. H. (1993) *Chem. Phys. Lipids 66*, 1−11.

Huang, C.-H. (1977) *Lipids 12*, 348−356.

Huang, T.-H., Lee, C. W. B., Das Gupta, S. K., Blume, A., & Griffin, R. G. (1993) *Biochemistry, 32*, 13277−13287.

Hui, S. W. (1993) *Cholesterol in Membrane Models* (Finegold, L., Ed.) Chapter 6, CRC Press, Boca Raton, FL.

Keough, K. M., Beynon, P., Oldfield, E., & Chapman, D. (1973) *Chem. Phys. Lipids 10*, 37−50.

Konikoff, F. M., Cohen, D. E., & Carey, M. C. (1994) *J. Lipid Res.* 35, 60−70.

Lala, A. K., Buttke, T. M., & Bloch, K. (1979) *J. Biol. Chem. 254*, 10582−10585.

Lazarevic, M. B., Skosey, J. L., Vitic, J., Mladenovic, V., Myones, B. L., Popovic, J., Swedler, W. I. (1993) *Semin. Arthritis Rheum. 23*, 99−103.
Le Guerneve, C., & Auger, M. (1995) *Biophys. J. 68*, 1952−1959.
Levecq, H., Barge, J., & Cerf, M. (1992) *Ann. Gastroenterol. Hepatol. 28*, 7−11.
Levin, I. W., Keihn, E., & Harris, W. C. (1985) *Biochim. Biophys. Acta 820*, 40−47.
Levine, Y. K. (1972) *Prog. Biophys. Mol. Biol. 24*, 1−74.
Li, K.-L., Tihal, C. A., Guo, M., & Stark, R. E. (1993) *Biochemistry 32*, 9926−9935.
Loomis, C. R., Shipley, G. G., & Small, D. M. (1979) *J. Lipid Res.* 20, 525.
Lund-Katz, S., & Phillips, M. C. (1981) *Biochem. Biophys. Res. Commun. 100*, 1735−1742.
McLaughlin, A. C., Cullis, P. R., Hemminga, M. A., Hoult, D. I., Radda, G. K., Ritchie, G. A., Seeley, P. J., & Richards, R. E. (1975) *FEBS Lett. 57*, 213−218.
McMullen, T. P. W., Lewis, R. N. A. H., & McElhaney, R. N. (1993) *Biochemistry 32*, 516−522.
McMullen, T. P. W., Lewis, R. N. A. H., & McElhaney, R. N. (1994) *Biophys. J. 66*, 741−752.
McMullen, T. P. W., Vilcheze, C., McElhaney, R. N., & Bittman, R. (1995) *Biophys. J. 69*, 169−176.
Monck, M. A., Bloom, M., Lafleur, M., Lewis, R. N. A. H., McElhaney, R. N., & Cullis, P. R. (1993) *Biochemistry 32*, 3081−3088.
Murari, R., Murari, M. P., & Baumann, W. J. (1986) *Biochemistry 25*, 1062−1067.
Oldfield, E., Adebodun, F., Chung, J., Montez, B., Park, K. D., Le, H., & Phillips, B. (1991) *Biochemistry 30*, 11025−11028.
Opella, S. J., Yesinowski, J. P., & Waugh, J. S. (1976) *Proc. Natl. Acad. Sci. U.S.A. 73*, 3812−3815.
Phillips, M. C. (1990) *Hepatology 12*, 75S−82S.
Phillips, M. C., & Finer, E. G. (1974) *Biochim. Biophys Acta 356*, 199−206.
Presti, F. T., Pace, R. J., & Chan, S. I. (1982) *Biochemistry 21*, 3831−3835.
Rajan, S., Kang S.-Y., Gutowsky, H. S., & Oldfield, E. (1981) *J. Biol. Chem. 256*, 1160−1166.
Ranadive, G. N., & Lala, A. K. (1987) *Biochemistry 26*, 22426−22431.
Robinson, A., Richard, W. G., Thomas, P. J., & Hann, M. M. (1995) *Biophys. J. 68*, 164−170.
Sankaram, M. B., & Thompson, T. E. (1990) *Biochemistry 29*, 10676−10684.
Sankaram, M. B., & Thompson, T. E. (1991) *Proc. Natl. Acad. Sci. U.S.A. 88*, 8686−8690.
Schmidt, C. F., Barenholz, Y., Huang, C., & Thompson, T. E. (1977) *Biochemistry 16*, 3948−3954.
Scott, H. L., & Cherng, S. L. (1977) *Biochim. Biophys. Acta 510*, 209−215.
Seelig, J., & Gally, U. H. (1976) *Biochemistry 15*, 5199.
Sefcik, M. D., Schaefer, J., Stejskal, E. O., & Mckay, R. A., Ellena, J. F., Dodd, S. W., & Brown, M. F. (1983) *Biochem. Biophys. Res. Commun. 114*, 1048−1055.
Senak, L., Moore, D., & Mendelsohn, R. (1992) *J. Phys. Chem. 96*, 2749−2754.
Siminovitch, D. J., Ruocco, M. J., Makriyannis, A., & Griffin, R. G. (1987) *Biochim. Biophys. Acta 901*, 191−200.
Slater, S. J., Ho, C., Taddeo, F. J., Kelly, M. B., & Stubbs, C. D. (1993) *Biochemistry 32*, 3714−3721.
Smith, S. O., Kustanovich, I., Bhamidipati, S., Salmon, A., & Hamilton, J. A. (1992) *Biochemistry 31*, 11660−11664.
Somjen, G. J., Lipka, G., Schulthess, G., Koch, M. H. J., Wachtel, E., Gilat, T., & Hauser, H. (1995) *Biophys. J. 68*, 2342−2349.
Swartz, G. M., Jr., Gentry, M. K., Amende, L. M., Blanchette-Mackie, E. J., & Alving, C. A. (1988) *Proc. Natl. Acad. Sci. U.S.A. 85*, 1902−1906.
Tangirala, R. K., Jerome, W. G., Jones, N. L., Small, D. M., Johnson, W. J., Glick, J. M., Mahlberg, F. H., & Rothblat, G. H. (1994) *J. Lipid Res. 35*, 93−104.
Taylor, M. G., Akiyama, T., & Smith, I. C. P. (1981) *Chem. Phys. Lipids 29*, 327−339.
Thomson, A. B., Schoeller, C., Keelan, M., Smith, L., & Clandinin, M. T. (1993) *Can. J. Physiol. Pharmacol. 71*, 531−555.
VanderHart, D. L. (1981) *J. Magn. Reson. 44*, 117−125.
Vist, M. R., & Davis, J. H. (1990) *Biochemistry 29*, 451−464.
Yeagle, P. L. (1988) *The Biology of Cholesterol* (Yeagle, P. L., Ed.) Chapter 6, CRC Press, Boca Raton, FL.
Yeagle, P. L., & Martin, R. B. (1976) *Biochem. Biophys. Res. Commun. 69*, 775−780.
Yeagle, P. L., Hutton, W., Huang, C.-H., & Martin, R. B. (1975) *Proc. Natl. Acad. Sci. U.S.A. 72*, 3477−3481.
Yeagle, P. L., Hutton, W., Huang, C.-H., & Martin, R. B. (1977) *Biochemistry 16*, 4344−449.
Wittebort, R. J., Schmidt, C. F., & Griffin, R. G. (1981) *Biochemistry 20*, 4223−4228.
Wong, P. T. T., Capes, S. E., & Mantsch, H. H. (1989) *Biochim. Biophys. Acta 980*, 37−41.
Worcester, D., & Franks, N. P. (1976) *J. Mol. Biol. 100*, 359.
Wu, W.-G., & Chi, L.-M. (1990) *Biochim. Biophys. Acta 1026*, 225−235.

BI9515735